Ultrathin crystalline-silicon solar cells with embedded photonic crystals

Shrestha Basu Mallick, Mukul Agrawal, Artit Wangperawong, Edward S. Barnard, Kaushal K. Singh et al.

Citation: Appl. Phys. Lett. **100**, 053113 (2012); doi: 10.1063/1.3680602
View online: http://dx.doi.org/10.1063/1.3680602
View Table of Contents: http://apl.aip.org/resource/1/APPLAB/v100/i5
Published by the American Institute of Physics.

Ultrathin crystalline-silicon solar cells with embedded photonic crystals

Shrestha Basu Mallick,[1,a)] Mukul Agrawal,[2] Artit Wangperawong,[3] Edward S. Barnard,[4] Kaushal K. Singh,[2] Robert J. Visser,[2] Mark L. Brongersma,[4] and Peter Peumans[5]
[1]*Department of Applied Physics, Stanford University, Stanford, California 94305, USA*
[2]*Applied Materials Inc., Santa Clara, California 94505, USA*
[3]*Department of Electrical Engineering, Stanford University, Stanford, California 94305, USA*
[4]*Geballe Laboratory for Advanced Materials, Stanford University, Stanford California 94305, USA*
[5]*IMEC, Kapeldreef 75, B-3001 Leuven, Belgium*

(Received 19 October 2011; accepted 11 January 2012; published online 31 January 2012)

Photonic crystals (PCs) can be used to trap light in thin-film solar cells to increase optical absorption. We fabricated ultrathin c-Si solar cells whose active layer was patterned into a two-dimensional PC with a square lattice of 450 nm diameter holes spaced at a period of 750 nm. The PC couples incident light into quasiguided modes and can be engineered to increase coupling and thus optimize optical absorption. Both short-circuit current and external quantum efficiency measurements show an enhancement in optical absorption, especially at longer wavelengths. Scanning photocurrent maps confirm the improved optical absorption in the PC regions. © *2012 American Institute of Physics*. [doi:10.1063/1.3680602]

Thin-film photovoltaics has the potential to reduce cost by reducing the amount of photoactive material required and allowing for the use of material of poorer quality by virtue of the shorter minority carrier diffusion lengths that are required to achieve efficient carrier collection. Crystalline Silicon (c-Si) is an attractive material for photovoltaic cells because of its natural abundance, nearly ideal band gap, and the possibility to leverage existing process and materials knowledge. However, a major drawback of thin-film c-Si cells is the poor optical absorption in the near-infrared spectral range requiring the use of very efficient light trapping techniques. Light trapping approaches based on wave optics in thin-film cells have attracted significant interest. Several groups have used photonic crystals (PCs) for this purpose.[1–10] The PC can be situated outside the active material or can be part of it. Here, we consider the case where the active layer is patterned into a two-dimensional (2D) PC. Such a thin slab PC supports leaky- or quasi-guided modes[11] into which incident radiation can couple. We have previously shown that patterning a 400 nm-thick layer of c-Si into a double-layer PC increases the integrated short-circuit current by a factor of 3 when compared to a planar slab of equivalent volume.[7]

Here, we report on the fabrication of an ultrathin c-Si cell where the active material is patterned into a square-lattice 2D PC with a period of 750 nm and hole diameter of 450 nm and demonstrate increased external quantum efficiency and photocurrent in the near infrared region of the solar spectrum. As shown in Ref. 7, significant enhancement in light absorption is obtained as compared to a planar slab for a wide range of periods and hole diameters. The devices were fabricated using silicon-on-insulator (SOI) substrates. The slab consists of a 90 nm-thick SiO_2 top layer, a 335 nm-thick c-Si layer, and a 400 nm-thick buried oxide (BOX) layer followed by a c-Si substrate. The PC extends through the top two layers but not to the BOX.

Rigorous-coupled wave analysis[12] was used to model the optical absorption in the structures. In Fig. 1(a), the active layer's absorption spectrum is shown as a function of wavelength for the unpatterned slab (blue, dashed line) and PC structure (green, solid line). The absorption spectrum of

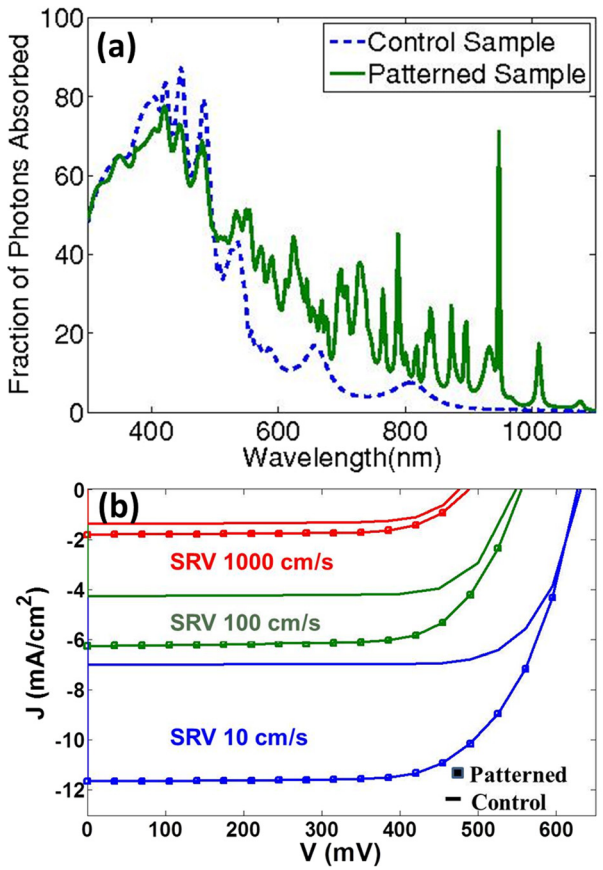

FIG. 1. (Color online) (a) Electromagnetic simulation of percentage of incident photons absorbed in the PC structure and a plain slab of similar thickness (b) Electrical simulations of device and reference cell with no PC for 3 different SRVs.

[a)]Electronic mail: sbasumal@stanford.edu.

the unpatterned slab is characterized by weak Fabry-Pérot resonances. The much sharper peaks in the absorption spectrum of the 2D PC are due to coupling of incident light into quasi-guided modes as discussed in Ref. 7. This enhancement in absorption is achieved despite the PC structure containing only 72% of the absorber volume of the planar slab.

Electrical simulations were performed using Sentaurus TCAD software. The total number of photons absorbed was calculated for the PC structure and the plain slab using the optical model discussed above and then plugged into the electrical model. We assume an effectively uniform carrier generation across the thickness. This is because the layer thickness is small compared to the absorption depth of light. The absorption length in silicon is approximately 500 nm at a wavelength of 450 nm. So our assumption of a uniform generation rate for a film of 335 nm is reasonable for a large part of the solar spectrum especially in the near IR which is where we wanted to show enhancement in absorption due to the PCs. Also, carrier diffusion over both the layer thickness and PC period is very fast compared to the carrier lifetime given that lifetimes in c-Si can be as long as 1msec. The surface recombination velocity (SRV) was assumed to be identical on all surfaces, including in the holes that make up the PC. Current-voltage (IV) curves were modeled for three different SRVs: 10, 100, and 1000 cm/s (Fig. 1(b)). The dominant bulk recombination mechanism was Shockley-Read-Hall and the bulk minority carrier lifetime was assumed to be 100 μs. Auger and trap-assisted Auger recombination effects were also included in the model, and a doping-dependent mobility model was used. The enhancement in short-circuit current density (J_{sc}) of the PC structure over the planar slab is 67% for SRV = 10 cm/s, 44% for SRV = 100 cm/s, and 29% for SRV = 1000 cm/s. Gains in J_{sc} are achieved even for relatively high SRVs (e.g., 1000 cm/s) which makes the experimental demonstration easier.[13] Thus, with the right PC design the absorption per unit cell of the PC is enhanced more than the recombination per unit cell is increased.

For the fabrication of the structures an SOI wafer with a 400 nm-thick p-type doped ($N_A = 10^{15}\,\mathrm{cm}^{-3}$) device layer was used. The cells were fabricated using a combination of photolithography and etching. Each cell had a 1 mm × 1 mm active area over which 2 μm-wide interdigitated p and n-doped regions were created at intervals of 50 μm to define p and n contacts (Fig. 2). The dopants (boron (B) and phosphorus (P)) were introduced using ion implantation and had Gaussian profiles with expected peak concentrations of $3.2 \times 10^{20}\,\mathrm{cm}^{-3}$. A 50 nm-thick thermal SiO_2 layer was then grown. The active cell area was subsequently patterned into the square lattice 2D PCs. An i-line step-and-repeat aligner was used to expose photoresist and CHF_3 dry etch-chemistry was used to transfer the pattern into the thermal SiO_2 layer. The c-Si layer was then etched using Cl_2/HBr chemistry using the SiO_2 as a masking layer.

After removal of the SiO_2 mask, all exposed surfaces (i.e., the c-Si top surface and the exposed surface in the etched holes) were passivated by growing a 30 nm-thick layer of thermal SiO_2 that serves as a passivation layer to reduce surface recombination at the Si surface and as a masking layer for the final step of patterning contact holes.

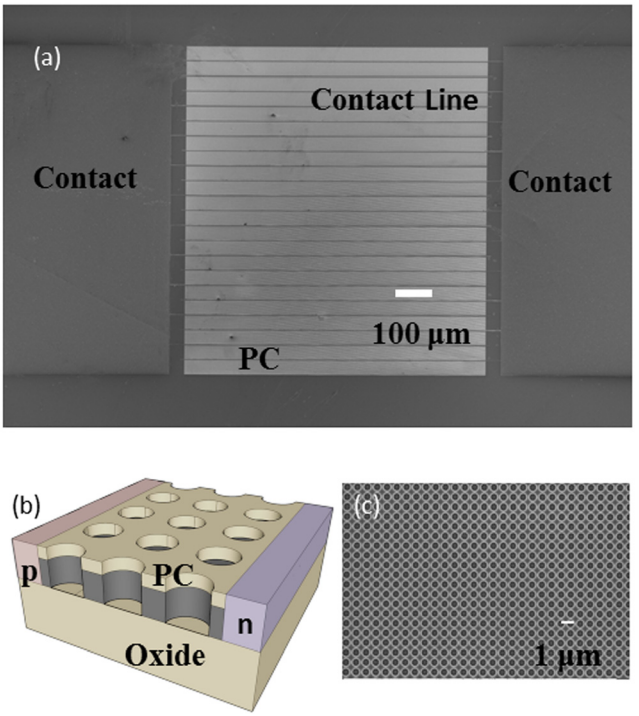

FIG. 2. (Color online) (a) SEM of fabricated device (b) Schematic of unit cell of the device (c) SEM close-up of region patterned into PC.

The contact holes are defined over the p and n-doped regions using a CHF3 dry etch. The final thickness of the active layer after the thermal oxide growth is 335 nm. Finally, a 300 nm-thick layer of Al:1%Si is sputtered and lithographically patterned into interdigitated fingers connected to opposing contact pads over the doped contact regions. A scanning electron microscope (SEM) image and a schematic of the fully fabricated structure are shown in Figs. 2(a) and 2(b). In Fig. 2(c)), a higher magnification image of the PC region is shown. The contact lines shade approximately 4% of the total area.

IV curves were measured for the device and a control sample using an AM1.5 solar simulator. The control sample is a planar slab of c-Si with the same contacts. The device and control sample were within a 1 cm distance from each other on the substrate to minimize processing-borne non-uniformities. The devices with a PC have a higher J_{sc} (2.05 mA/cm^2) compared to the control sample (1.6 mA/cm^2). We assume that poor passivation, fabrication inaccuracies, and contamination during fabrication are some of the major reasons for the poor performance.

External quantum efficiency (EQE) measurements were done to determine the wavelength-dependent absorption. These measurements were done with a beam diameter of ~0.75 mm which fell entirely within the device area. Because of possible shadowing effects by the contacts, the EQE data were multiplied by the J_{sc} ratios. The presence of the PC (green, solid line) leads to a considerable improvement in EQE for longer wavelengths as compared to the planar slab (blue, dashed line), as shown in Fig. 3. Furthermore, the large number of narrow peaks indicates the presence of quasi-guided modes.

Laser-scanning photocurrent measurements were performed using a 10 μm laser spot at $\lambda = 1000$ nm (see Fig. 4). The region structured like a PC shows significantly higher

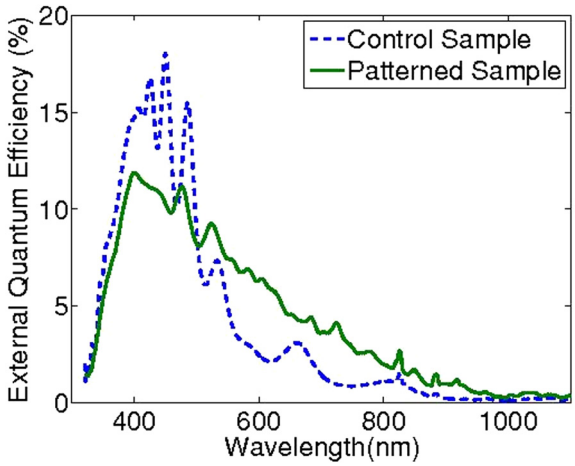

FIG. 3. (Color online) Normalized EQE data for a PC and reference unpatterned device that shows enhanced photocurrent in the near IR.

photocurrent compared to the plain unstructured region between the contact and the PC. The color scale indicates the current normalized to the average current in the plain region and the PC region is shown to generate a photocurrent

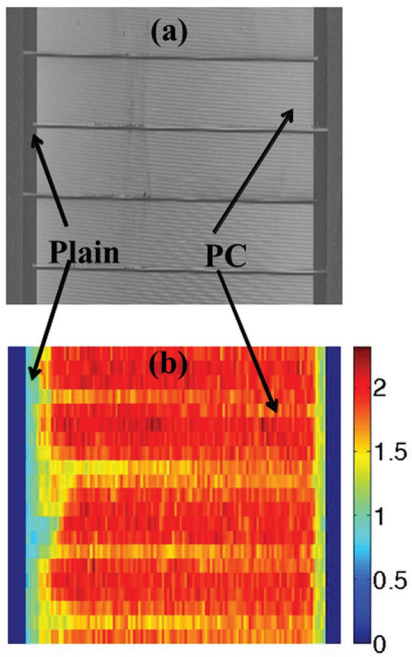

FIG. 4. (Color) (a) SEM image of a portion of the PC structure (b) Laser scanned photocurrent image of the same portion at a wavelength of 1000 nm. The aspect ratios of the SEM image have been altered to highlight the correspondence between the SEM and the photocurrent image. The scale shows current normalized to current in the plain region.

greater than two times the current in the plain region. The observed enhancement scanning photocurrent measurement at $\lambda = 1000$ nm is larger than that expected from the simulation. This is possibly due to differences between the simulation and the fabrication such as for example between the simulated etch profiles (straight) and the fabricated etch profiles (slightly sloping).

In conclusion, we have demonstrated an ultrathin c-Si solar cell where the device layer is patterned into a 2D PC. The resulting PC device clearly shows enhanced absorption in the near-infrared in agreement with optical modeling. This was designed as a proof-of-concept experiment to demonstrate the benefits of patterning a PC into the active layer of a solar cell so it was not optimized for cost. However, to fully utilize the potential of the small film thicknesses which allow for lower cost, poorer quality material, architectures in which the film is contacted from top and bottom need to be developed. The cell should have the thin silicon film on a low cost substrate, the PCs should be patterned using a low cost technique and better anti-reflective coatings and back reflectors should be incorporated in the design.

We thank N. Sergeant, E. Pickett, and U. Aboudi for valuable discussion and help. We acknowledge support from Applied Materials, Inc. and the Department of Energy grant DE-FG02-07ER46426.

[1]B. M. Kayes, H. A. Atwater, and N. S. Lewis, J. Appl. Phys. **97**, 114302 (2005).
[2]P. Bermel, C. Luo, L. Zeng, L. C. Kimerling, and J. D. Joannopoulos, Opt. Express **15**(25), 16986 (2007).
[3]P. G. O'Brien, N. P. Kherani, A. Chutinan, G. A. Ozin, S. John, and S. Zukotynski, Adv. Mater. **20**(8), 1577 (2008).
[4]R. Biswas, J. Bhattacharya, B. Lewis, N. Chakravarty, and V. Dalal, Solar Energy Materials and Solar Cells **94**(12), 2337 (2010).
[5]A. Bielawny, C. Rockstuhl, F. Lederer, and R. B. Wehrspohn, Opt. Express **17**(10), 8439 (2009).
[6]Y.-C. Lee, C.-F. Huang, J.-Y. Chang, and M.-L. Wu, Opt. Express **16**(11), 7969 (2008).
[7]A. Chutinan, N. P. Kherani, and S. Zukotynski, Opt. Express **17**(11), 8871 (2009).
[8]S. B. Mallick, M. Agrawal, and P. Peumans, Opt. Express **18**(6), 5691 (2010).
[9]O. El Daif, E. Drouard, G. Gomard, A. Kaminski, A. Fave, M. Lemiti, S. Ahn, S. Kim, P. Cabarrocas, H. Jeon, and C. Seassal, Opt. Express **18**(3), A293 (2010).
[10]X. Meng, G. Gomard, O. El Daif, E. Drouard, R. Orobtchouk, A. Kaminski, A. Fave, M. Lemiti, A. Abramov, P. Cabarrrocas, and C. Seassal, Sol. Energy Mater. Solar Cells **95**(1), 32 (2011).
[11]S. G. Tikhodeev, A. L. Yablonskii, E. A. Muljarov, N. A. Gippius, and T. Ishihara, Phys. Rev. B **66**(4), 045102 (2002).
[12]M. G. Moharam, E. B. Grann, D. A. Pommet, and T. K. Gaylord, J. Opt. Soc. Am. A **12**(5), 1068 (1995).
[13]A. G. Aberle, Prog. Photovoltaics **8**(5), 473 (2000).